Electronic Supplementary Material (ESI) for CrystEngComm

Supporting Information for

Stepwise Pillar Insertion into Metal-Organic Frameworks: A Sequential–Assembly Approach

Brandon J. Burnett[a] *and Wonyoung Choe*[a,b,*]

[a] Department of Chemistry, University of Nebraska-Lincoln, Lincoln, Nebraska, 685188-0304, United States, [b] School of Nano-Bioscience and Chemical Engineering, Ulsan National Institute of Science and Technology (UNIST), 50 UNIST Road, Ulsan 689-798, Korea

*To whom correspondence should be addressed. E-mail: chem571@gmail.com

1. Experimental

1.1 General Considerations

Materials. 5,10,15,20-tetrakis(4-carboxyphenyl)-21*H*,23*H*-porphyrin (TCPP) (Frontier Scientific), $Zn(NO_3)_2 \cdot 6H_2O$ (Sigma-Aldrich), Pyrazine (Sigma-Aldrich), *4,4'*-bipyridine (BPY) (Sigma-Aldrich), 3,6-di-(4-pyridyl)-1,2,4,5-tetrazine (DPT) (TCI America), and *N*,*N*-diethylformamide (DEF) (TCI America) were all obtained from commercial sources and used without further purification. *N*,*N*'-di-(4-pyridyl)-1,4,5,8-napthalenetetracarboxydiimide (DPNI) was synthesized according to published procedure.[1]

Instrumentation. X-ray diffraction data were taken using a spinning capillary method[2] with a Bruker AXS DA x-ray diffractometer with a GADDS area detector and a conventional copper target x-ray tube set to 40 KV and 40 mA. The resulting patterns were compared to the simulated patterns obtained by Mercury.[3] Thermogravimetric Analysis (TGA) was performed on a Perkin Elmer STA 6000 Termogravimetric Analyzer, heated from 25°C to 600°C at a rate of 5°C/minute under N_2 atmosphere. ^{1}H NMR was performed on a Bruker FT-NMR spectrometer (300 MHz).

1.2 Syntheses. For all structures, TGA and Elemental Analysis revealed the amount of solvent in the crystals and were taken into account to calculate the yield.

PPF-1[Zn_2(ZnTCPP)]. TCPP (55.3 mg, 0.07 mmol), $Zn(NO_3)_2 \cdot 6H_2O$ (62.3 mg, 0.21 mmol), and pyrazine (11.2 mg, 0.14 mmol) were added to a mixture of DEF (10.5 mL) and ethanol (3.5 mL) in a capped pressure vessel, sonicated to mix, and heated to 80°C for 24 h, followed by slow cooling to room temperature over 9 h. Yield: 73.3 mg (71% based on porphyrin). Anal. Calcd. for $[C_{48}H_{24}N_4O_8Zn_3]$ 3.3 DEF ·1.5 H_2O · ethanol · 0.4 pyrazine: C, 57.7; H, 5.0; N, 8.9%. Found: C, 57.8; H, 5.0; N, 9.0%.

PPF-27 [Zn_2(ZnTCPP)(BPY)] from PPF-1. Filtered PPF-1 (44.1 mg, 0.03 mmol) and BPY (3.2 mg, 0.02 mmol) were added to a mixture of DEF (4.5 mL) and ethanol (1.5mL) in a capped vial, swirled by hand to mix, and left to react at room temperature for ~ 2 hr. Yield: 45.1 mg (95%). Anal. Calcd. for $[C_{58}H_{32}N_6O_8Zn_3]$ 3DEF · 2 H_2O · 1 ethanol · 0.2 BPY: C, 59.5; H, 5.0; N, 9.0%. Found: C, 59.4; H, 5.0; N, 9.0%.

PPF-18 [Zn_2(ZnTCPP)(DPNI)] from PPF-1. Filtered PPF-1 (14.7 mg, 0.01 mmol) and DPNI (8.5 mg, 0.02 mmol) were added to a mixture of DEF (1.5 mL) and ethanol (0.5 mL) in a capped vial, swirled by hand to mix, and left to react at room temperature for ~ 2 hr. Yield: 21.2 mg (86%). Anal. Calcd. for $[C_{72}H_{36}N_8O_{12}Zn_3]$ 3.6 DEF · 0.5 H_2O · 3.0 ethanol · 0.2 pyrazine: C, 59.0; H, 4.9; N, 9.0%. Found: C, 59.0; H, 4.9; N, 9.0%.

PPF-21 [Zn_2(ZnTCPP)(DPT)] from PPF-1. Filtered PPF-1 (14.7 mg, 0.01 mmol) and DPT (4.6 mg, 0.02 mmol) were added to a mixture of DEF (1.5 mL) and ethanol (0.5 mL) in a

capped vial, swirled by hand to mix, and left to react at room temperature for ~2 hr. Yield: 16.8 mg (89%). Anal. Calcd. for $[C_{60}H_{32}N_{10}O_8Zn_3]$ 1.7 DEF · 2.8 ethanol: C, 58.6; H, 4.49; N, 10.8%. Found: C, 58.8; H, 4.52; N, 10.7%.

PPF-4 $[Zn_2(ZnTCPP)(BPY)_{1.5}]$ from PPF-27. Filtered PPF-27 (15.8 mg, 0.01 mmol) and BPY (8.0 mg, 0.05 mmol) were added to a mixture of DEF (1.5 mL) and ethanol (0.5 mL) in a capped vial, swirled by hand to mix, and left to react at room temperature for ~2 hr. Yield: 15.0 mg (92%). Anal. Calcd. for $[C_{63}H_{36}N_7O_8Zn_3]$ 3.3 DEF · 1.5 H_2O · 1 ethanol: C, 60.3; H, 5.1; N, 8.9%. Found: C, 61.0; H, 5.4; N, 8.9%.

PPF-4 from PPF-1. Filtered PPF-1 (14.7 mg, 0.01 mmol) and BPY(8.0 mg, 0.05 mmol) were added to a mixture of DEF(1.5 mL) and ethanol (0.5 mL) in a capped vial, swirled by hand to mix, and left to react at room temperature for ~2 hr. Purity of PPF-4 was confirmed by PXRD.

PPF-27 from PPF-18. Filtered PPF-18 (24.5 mg, 0.01 mmol) and BPY (3.2 mg, 0.02 mmol) were added to a mixture of DEF(1.5 mL) and ethanol (0.5 mL) in a capped vial, swirled by hand to mix, and left to react at room temperature for ~2 hr. Purity of PPF-27 was confirmed by PXRD.

PPF-27 from PPF-21. Filtered PPF-21 (18.9mg, 0.01 mmol) and BPY (3.2 mg, 0.02 mmol) were added to a mixture of DEF (1.5 mL) and ethanol (0.5 mL) in a capped vial, swirled by hand to mix, and left to react at room temperature for ~2 hr. Purity of PPF-27 was confirmed by PXRD.

2. Structure Analysis

2.1 Analysis of PPF-1

PPF-1 is synthesized using pyrazine as a directing agent, aiding in the AB stacking pattern observed by powder and single crystal X-ray diffraction spectrum. Without pyrazine in the experimental procedure, a different phase is observed in the powder X-ray diffraction spectrum. Thus it is believed that pyrazine is needed for the construction of the AB stacked PPF-1 structure. Pyrazine, however was not observed in the single crystal structure and elemental analysis indicates only 0.4 pyrazine molecules per unit cell indicating it being a guest molecule instead of a coordinated linker. To quantitatively find how much pyrazine was in PPF-1 structure, we digested samples of PPF-1 in acid according to the method reported by Cohen.[4] Approximately 5 mg of PPF-1 crystals were filtered, washed ≥ 3 times with 5 mL of DMF to rid the crystals of any free (unbound) ligands, and dried under vacuum at 90°C overnight. The dried crystals were then digested with sonication in 500 μL of dilute DCl (10 μL of 35% DCl in D_2O diluted with 500 μL of DMSO-d_6). ^{1}H NMR spectra was obtained from the resulting solution (Figure S3). Analysis of the integration of porphyrin signals to pyrazine signals indicate a porphyrin to pyrazine ratio of 1:0.3 which supports the conclusion that pyrazine is a guest and not a coordinated linker which would yield a porphyrin to pyrazine ratio of 1:1.

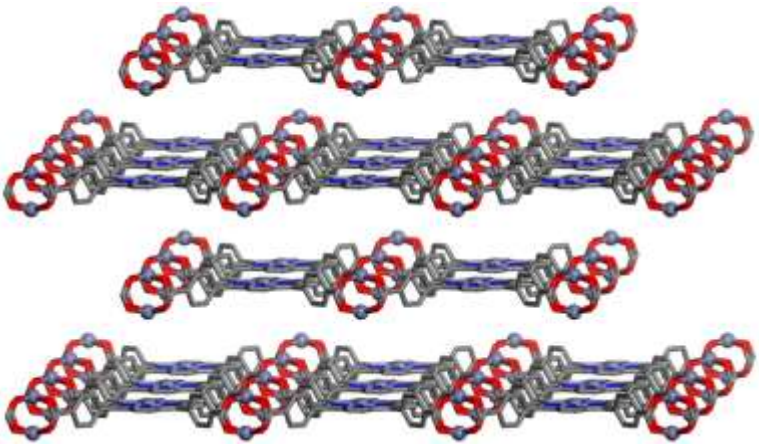

Figure S1. Representation of single crystal of PPF-1.

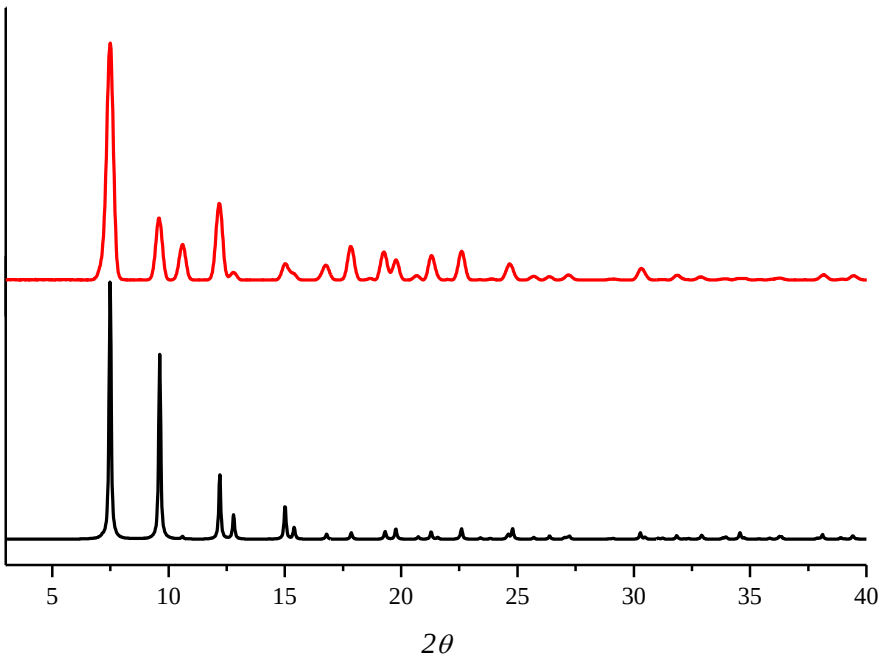

Figure S2. The simulated (black) and as synthesized (red) X-ray powder diffraction patterns for PPF-1.

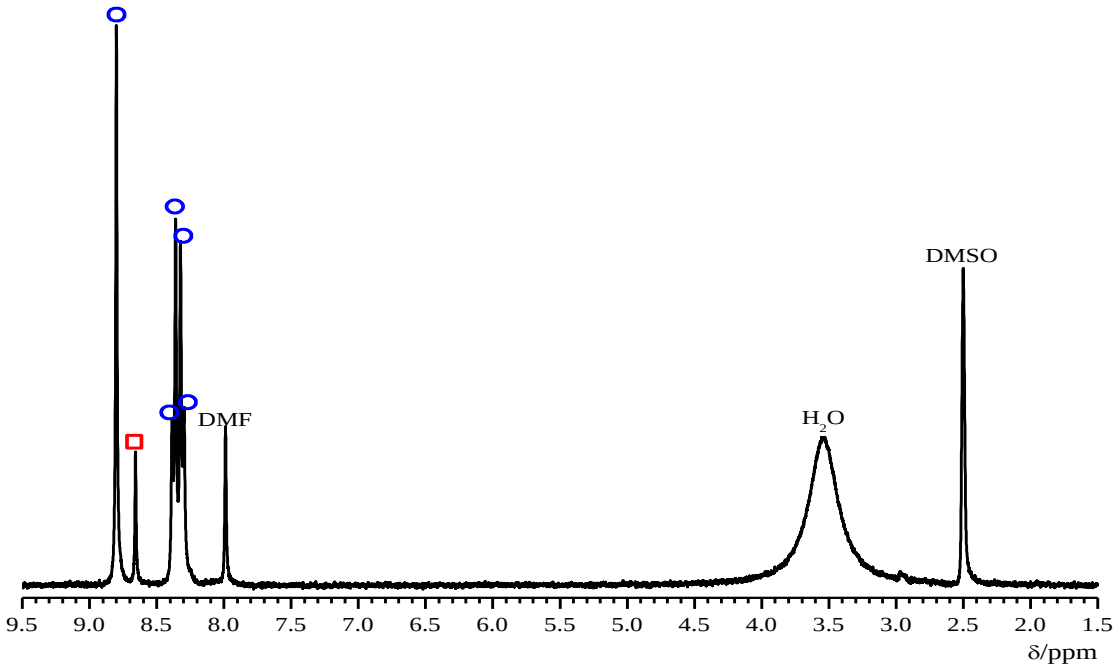

Figure S3. ^{1}H NMR spectra of digested PPF-1. Red squares and blue circles represent signals of pyrazine and ZnTCPP respectively.

2.2 Analysis of PPF-27 synthesized from PPF-1

Powder X-ray diffraction shows full conversion from PPF-1 to PPF-27 and no other products formed (Figure S5). To quantitatively find the occupation of BPY linker in PPF-27, we digested samples of PPF-27 in acid following the same method described above. Analysis of the ^{1}H NMR spectra shows 93% occupation of BPY linker in PPF-27 (Figure S6).

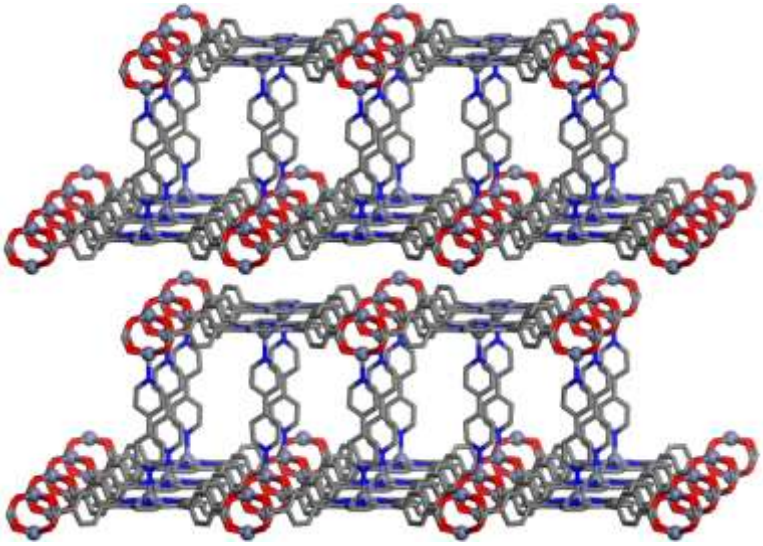

Figure S4. Representation of single crystal structure of PPF-27.

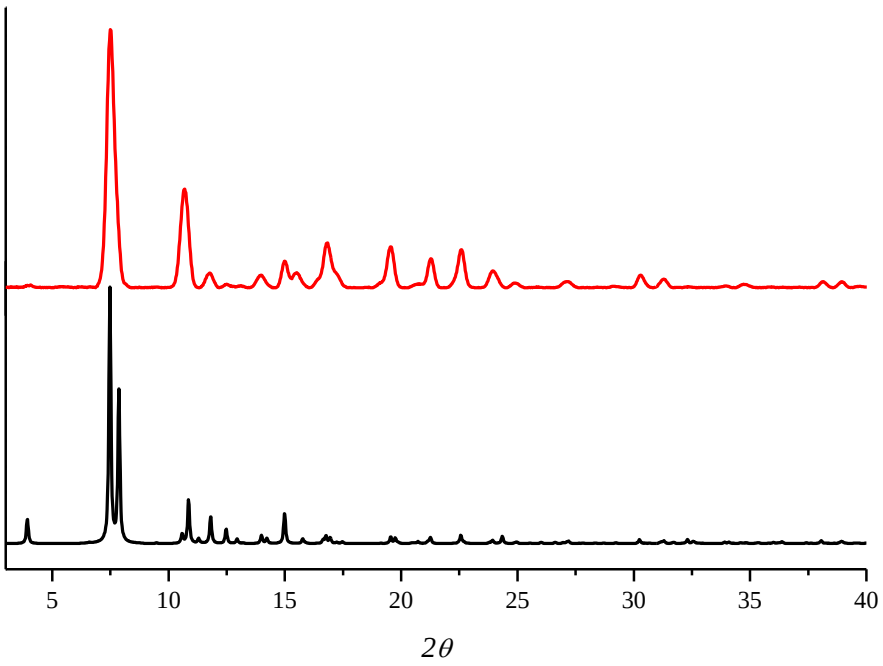

Figure S5. The simulated (black) and as synthesized (red) X-ray powder diffraction patterns for PPF-27.

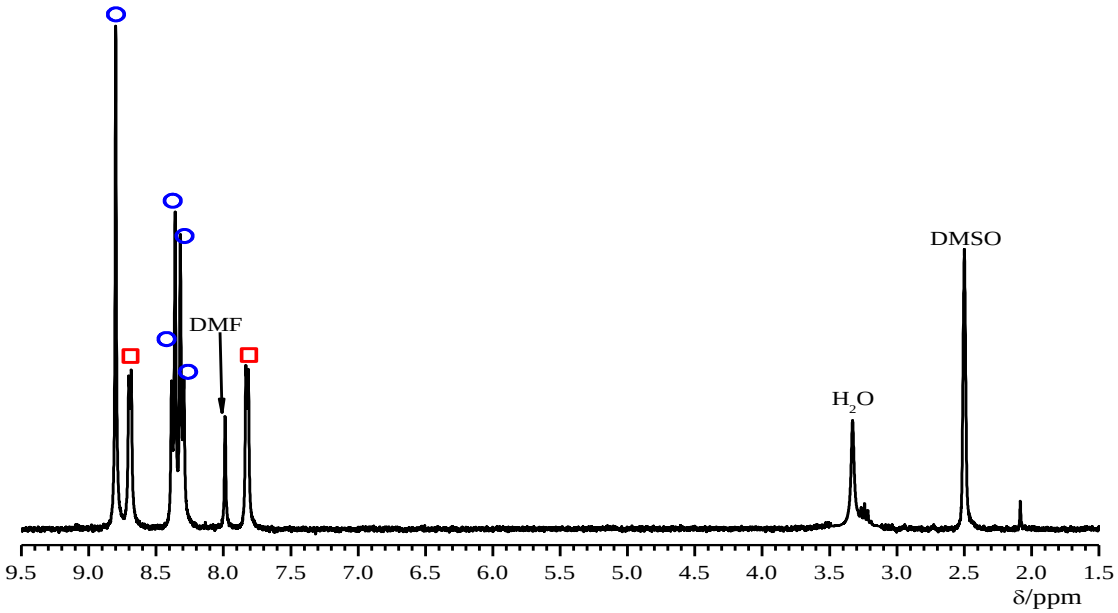

Figure S6. ^{1}H NMR spectra of digested PPF-27. Red squares and blue circles represent signals of BPY and ZnTCPP respectively.

2.3 Analysis of PPF-18 synthesized from PPF-1

Powder X-ray diffraction shows full conversion from PPF-1 to PPF-18 and no other products formed (Figure S8). To quantitatively find the occupation of DPNI linker in PPF-18, we digested samples of PPF-18 in acid following the same method described above. Analysis of the ^{1}H NMR spectra shows 89% occupation of DPNI linker in PPF-18 (Figure S9).

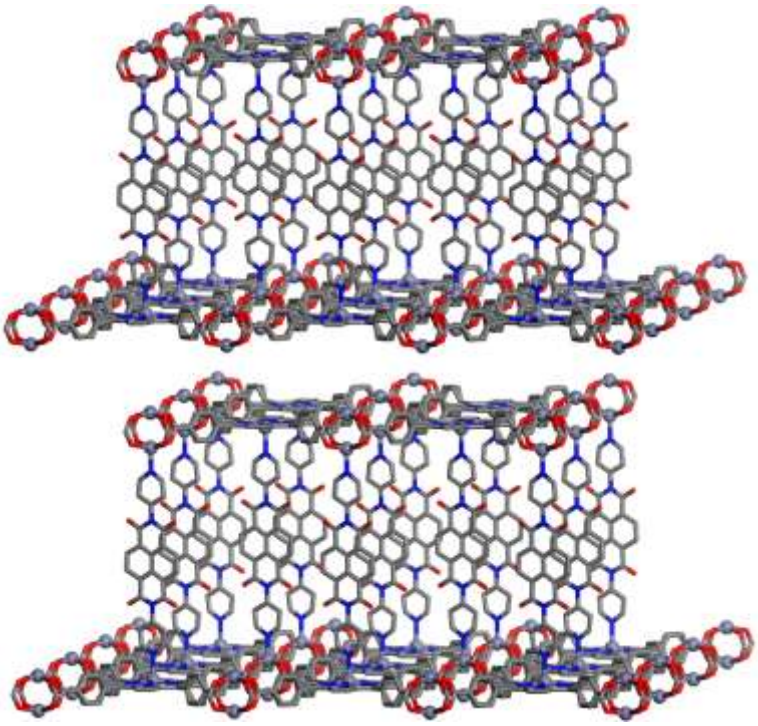

Figure S7. Representation of single crystal structure of PPF-18.

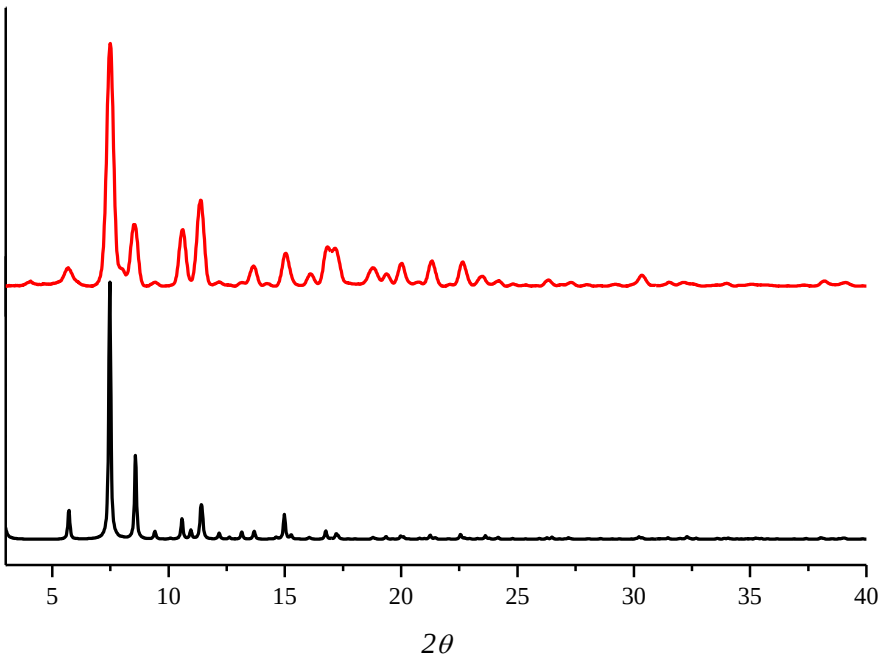

Figure S8. The simulated (black) and as synthesized (red) X-ray powder diffraction patterns for PPF-18.

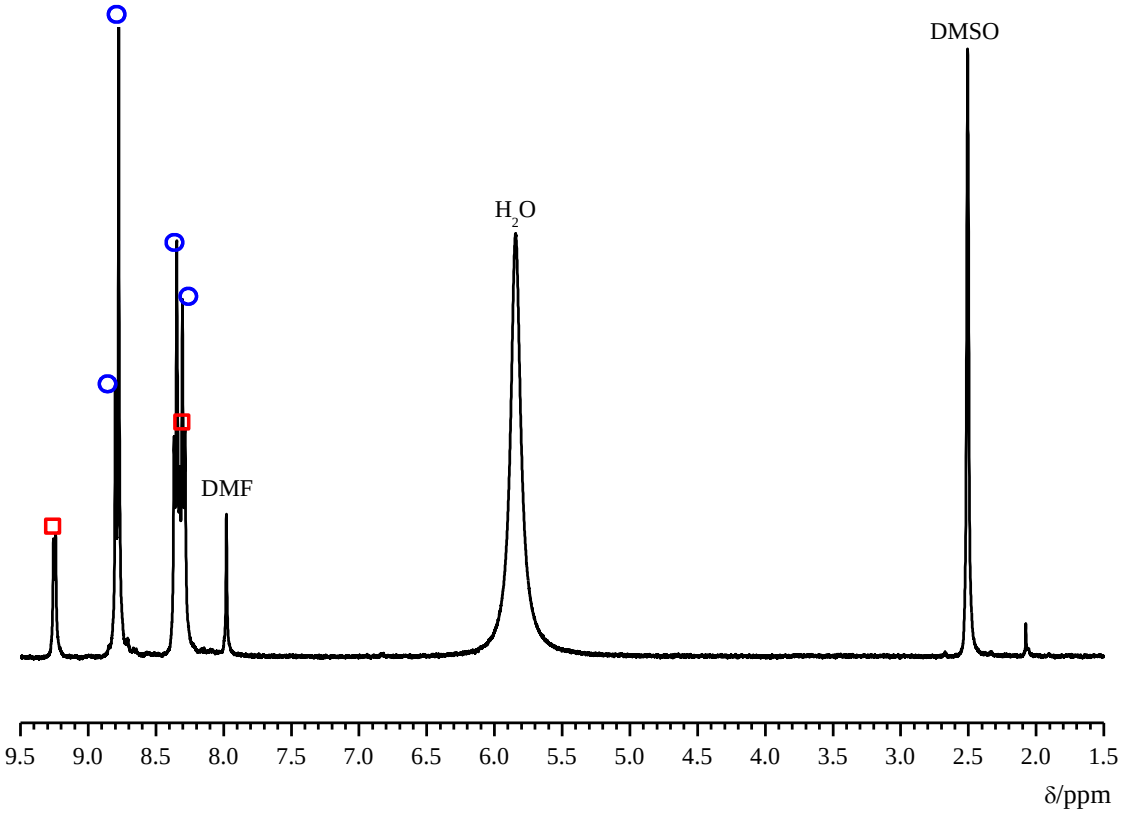

Figure S9. ^{1}H NMR spectra of digested PPF-18. Red squares and blue circles represent signals of DPNI and ZnTCPP respectively.

2.4 Analysis of PPF-21 synthesized from PPF-1

Powder X-ray diffraction shows full conversion from PPF-1 to PPF-21 and no other products formed (Figure S11). To quantitatively find the occupation of DPT linker in PPF-21, we digested samples of PPF-21 in acid following the same method described above. Analysis of the ^{1}H NMR spectra shows 87% occupation of DPT linker in PPF-21 (Figure S12).

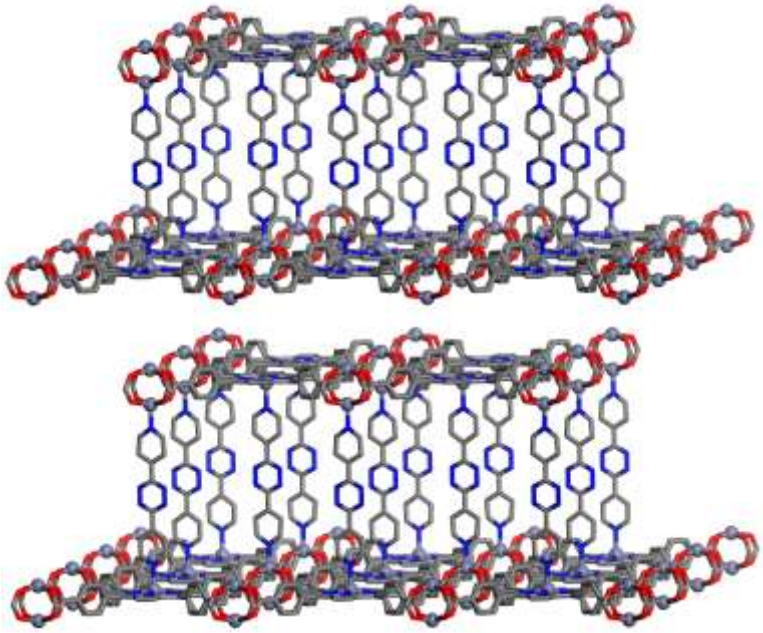

Figure S10. Representation of single crystal structure of PPF-21.

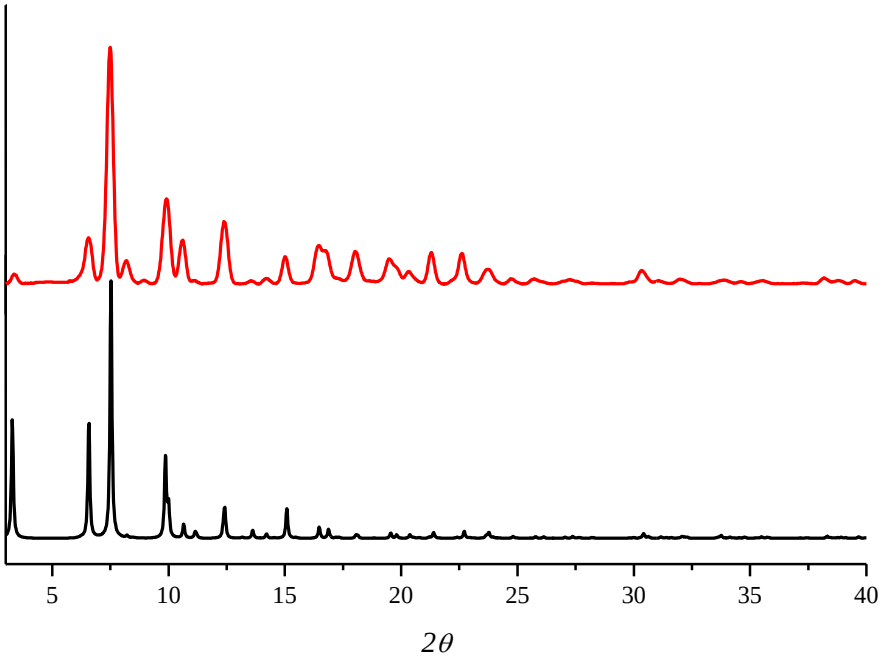

Figure S11. The simulated (black) and as synthesized (red) X-ray powder diffraction patterns for PPF-21.

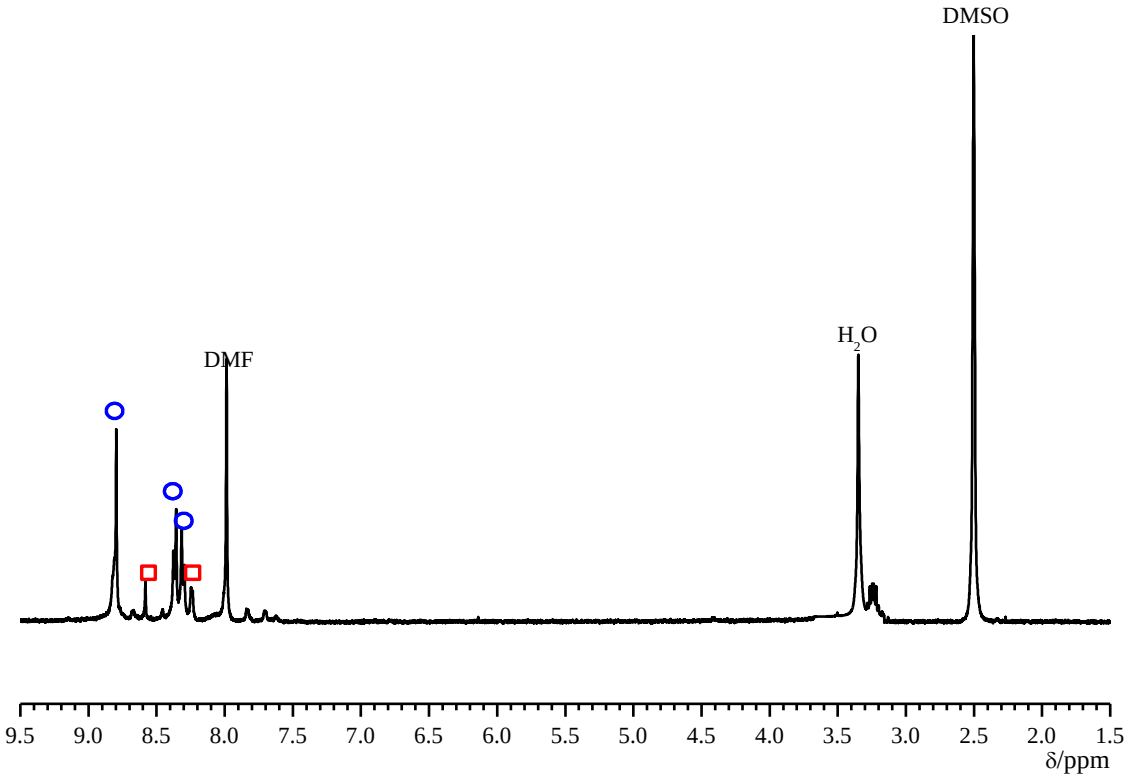

Figure S12. ^{1}H NMR spectra of digested PPF-21. Red squares and blue circles represent signals of DPT and ZnTCPP respectively.

2.5 Analysis of PPF-4 synthesized from PPF-27

Powder X-ray diffraction shows full conversion from PPF-27 to PPF-4 and no other products formed (Figure S14). To quantitatively find the occupation of BPY linker in PPF-4, we digested samples of PPF-4 in acid following the same method described above. Analysis of the ^{1}H NMR spectra shows 95% occupation of BPY linker in PPF-4 (Figure S15).

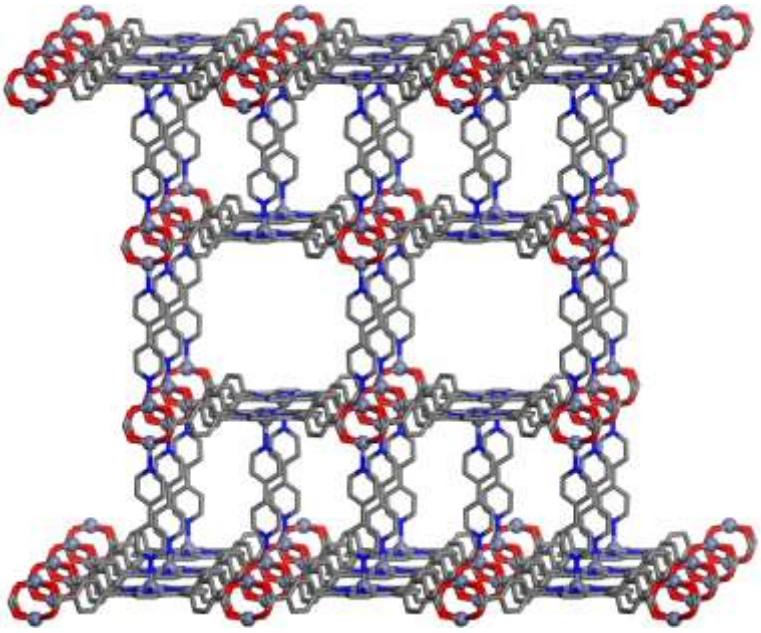

Figure S13. Representation of single crystal structure of PPF-4.

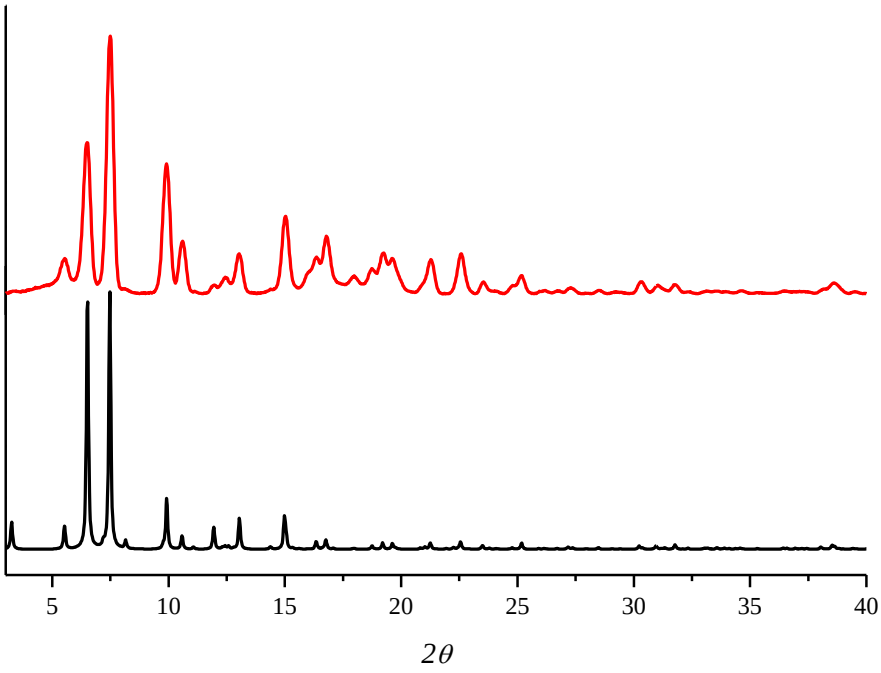

Figure S14. The simulated (black) and as synthesized (red) X-ray powder diffraction patterns for PPF-4.

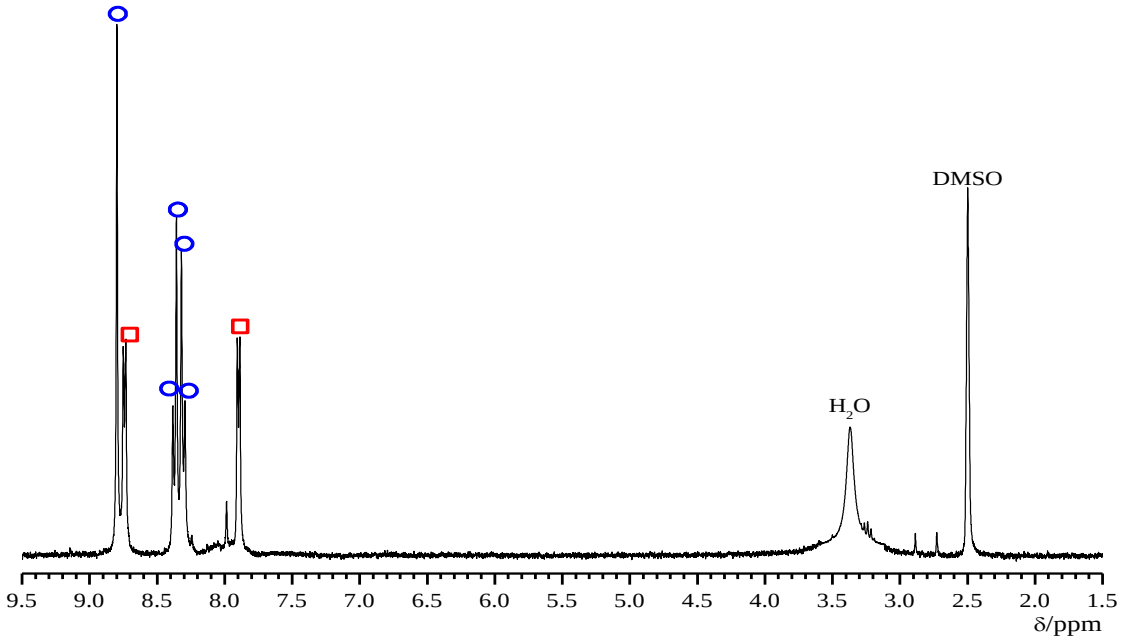

Figure S15. ^{1}H NMR spectra of digested PPF-4. Red squares and blue circles represent signals of BPY and ZnTCPP respectively.

2.6 Analysis of PPF-4 synthesized by PPF-1

Powder X-ray diffraction shows full conversion from PPF-1 to PPF-4 and no other products formed (Figure S16). To quantitatively find the occupation of BPY linker in PPF-4, we digested samples of PPF-4 in acid following the same method described above. Analysis of the ^{1}H NMR spectra shows 90% occupation of BPY linker in PPF-4 (Figure S17).

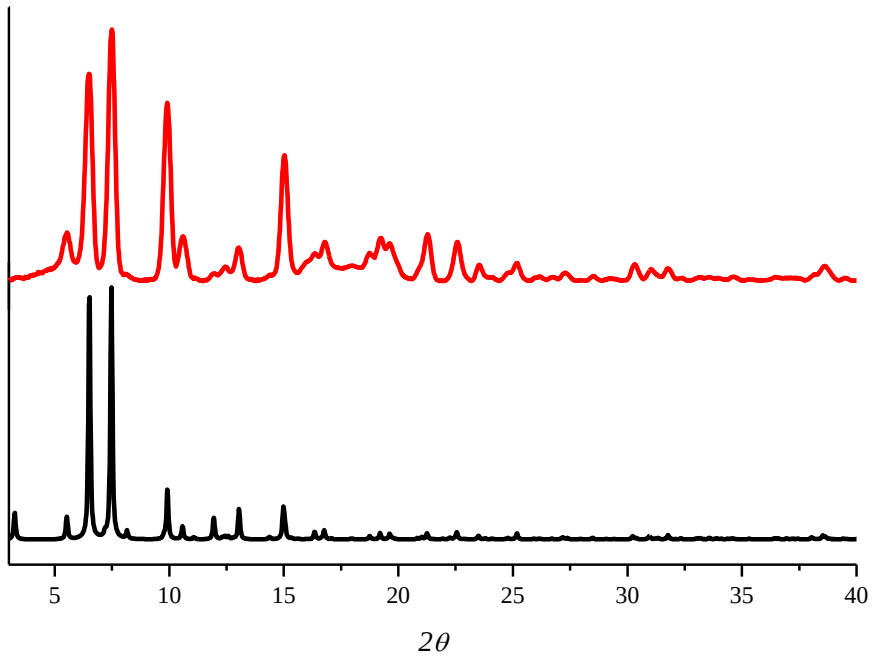

Figure S16. The simulated (black) and as synthesized (red) X-ray powder diffraction patterns for PPF-4.

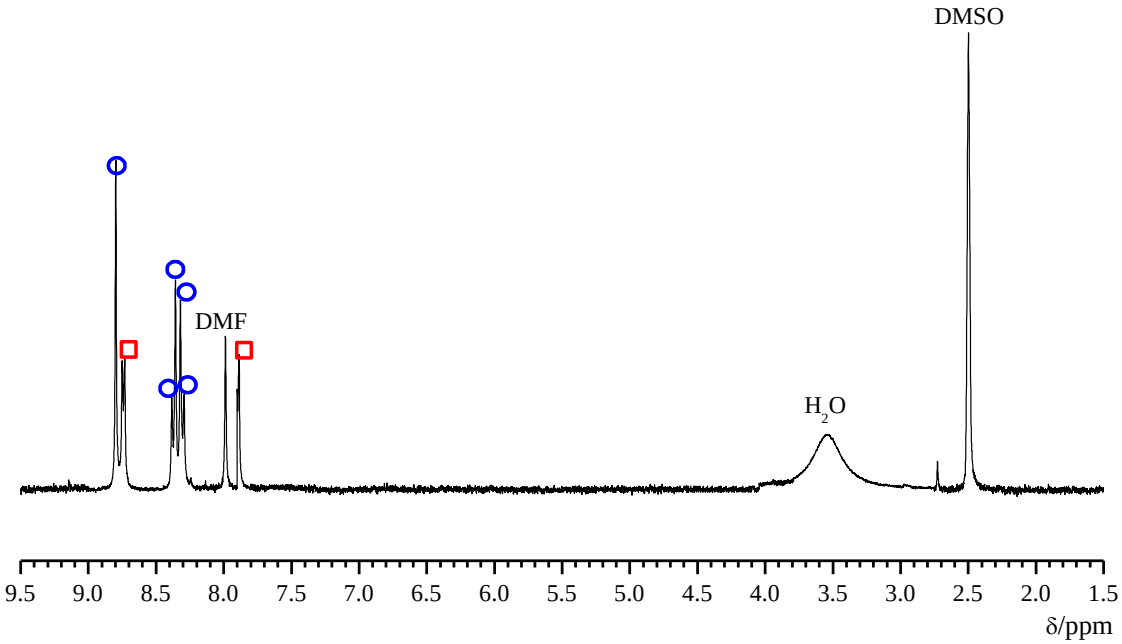

Figure S17. ^{1}H NMR spectra of digested PPF-4. Red squares and blue circles represent signals of BPY and ZnTCPP respectively.

Table S1. Amounts of reactants and resulting structures for the linker insertion investigation of PPFs.

Starting Structure	Pillar	Pillar Amt. (equivalents)	Phase(s) identified[a]
PPF-1	BPY	0.8	PPF-1 + PPF-27
PPF-1	BPY	1.0	PPF-1 + PPF-27
PPF-1	BPY	2.0	PPF-27
PPF-1	BPY	4.0	PPF-27 + PPF-4
PPF-1	BPY	5.0	PPF-4
PPF-1	DPNI	1.0	PPF-1 + PPF-18
PPF-1	DPNI	2.0	PPF-18
PPF-1	DPNI	5.0	PPF-18
PPF-1	DPT	1.0	PPF-1 + PPF-21
PPF-1	DPT	2.0	PPF-21
PPF-1	DPT	5.0	PPF-21
PPF-27	BPY	1.0	PPF-27
PPF-27	BPY	2.0	PPF-27
PPF-27	BPY	4.0	PPF-27 + PPF-4
PPF-27	BPY	5.0	PPF-4
PPF-18	DPNI	5.0	PPF-18
PPF-21	DPT	5.0	PPF-21
PPF-18	BPY	2.0	PPF-27
PPF-21	BPY	2.0	PPF-27

[a] based upon powder XRD pattern analysis

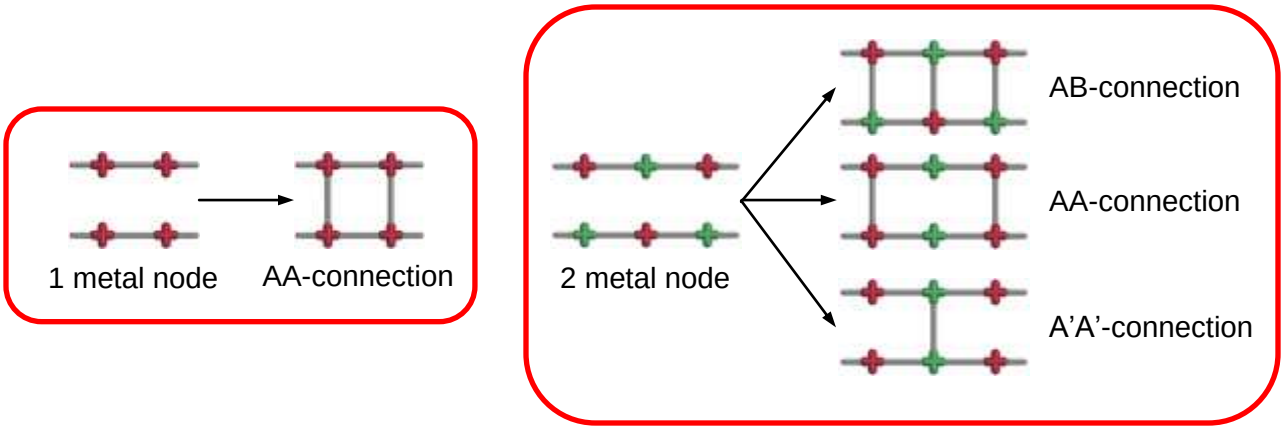

Figure S18. The difference in linker insertion connectivity between frameworks with one single metal node and two different metal nodes.

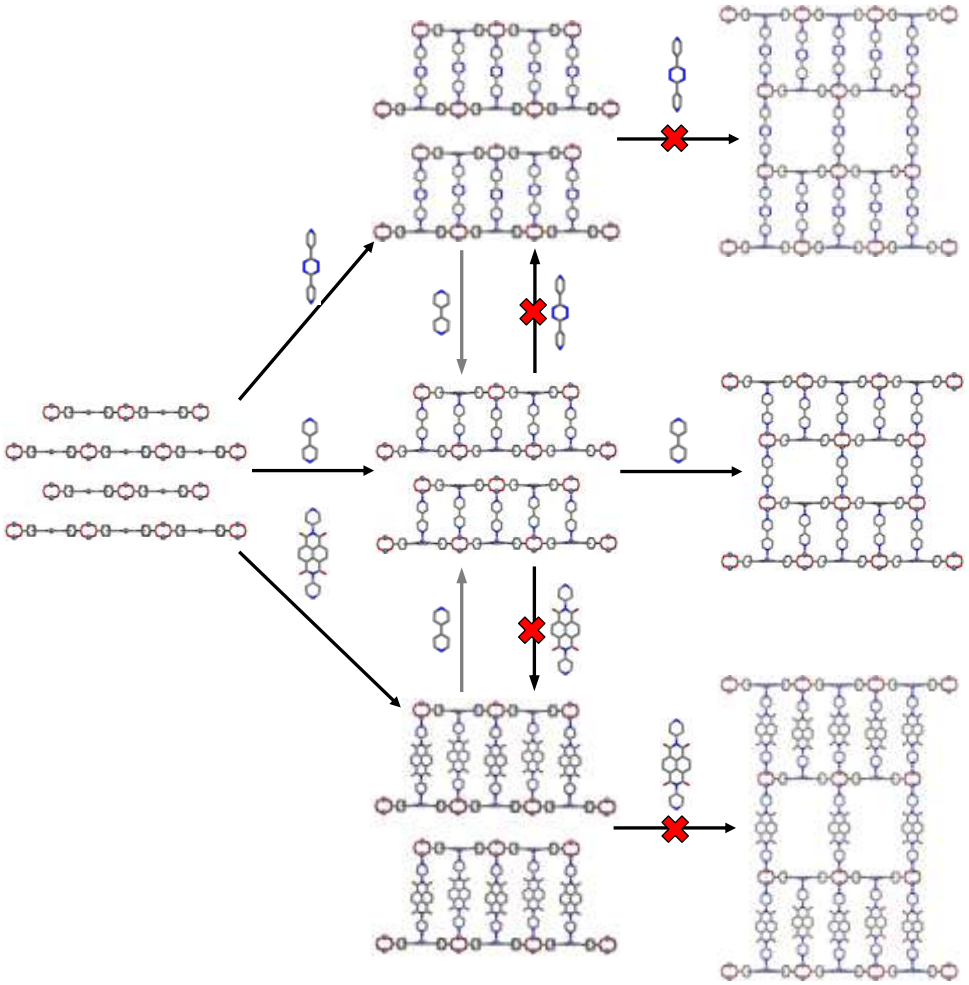

Figure S19. Schematic representation of all attempted linker insertion reactions in PPFs. Red crosses denote reactions which were not successful. Grey arrows denote a linker replacement reaction which was previously reported by our group (see ref. 2a).

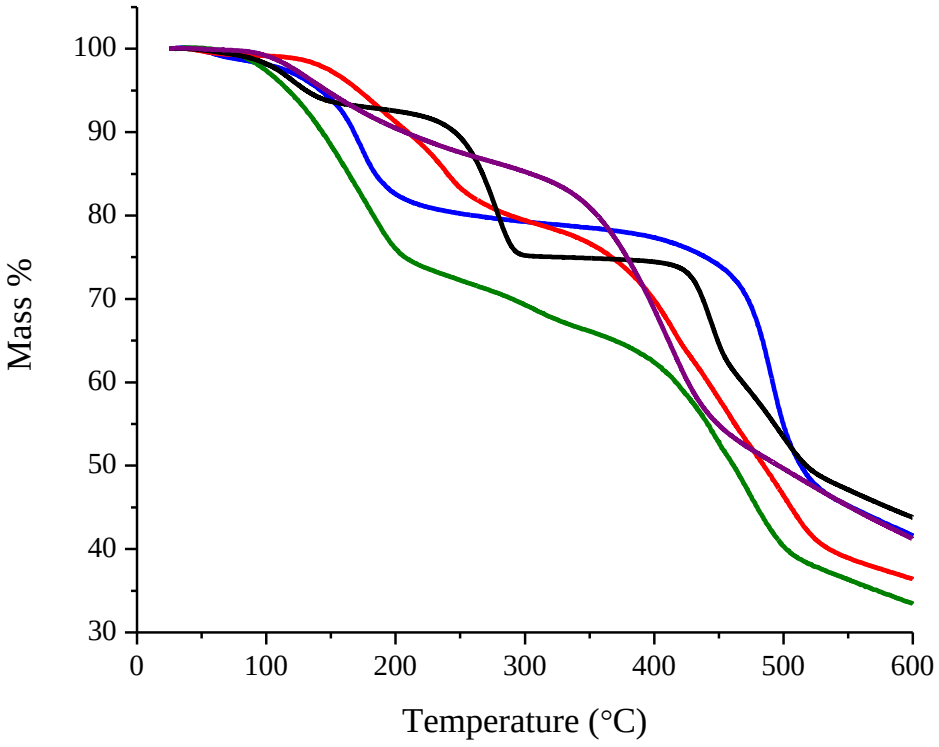

Figure S20. TGA data of PPF-1 (black), PPF-27 (red), PPF-18 (blue), PPF-21 (green), and PPF-4 (purple).

References

(1) Chung, H.; Barron, P. M.; Novotny, R. W.; Son, H. –T.; Hu, C.; Choe, W. *Cryst. Growth Des.* **2009**, *9*, 3327.

(2) (a) Burnett, B. J.; Barron, P. M.; Hu, C.; Choe, W. *J. Am. Chem. Soc.* **2011**, *133*, 9984. (b) Farha, O. K.; Sultz, A. M.; Sargeant, A. A.; Nguyen, S. T.; Hupp, J. T. *J. Am. Chem. Soc.* **2011**, *133*, 5652.

(3) http://www.ccdc.cam.ac.uk/products/mercury/

(4) Wang, Z.; Tanabe, K. K.; Cohen, S. M. *Inorg. Chem.* **2009**, *48*, 296.